Article ID: 1006-8775(2017) 02-0155-11

MICROSTRUCTURES AND TEMPORAL VARIATION CHARACTERISTICS DURING A SEA FOG EVENT ALONG THE WEST COAST OF THE TAIWAN STRAIT

ZHANG Yue (张 悦)[1, 2], FAN Shu-xian (樊曙先)[1, 3], ZHANG Shu-ting (张舒婷)[3], WEI Jin-cheng (魏锦成)[4]
(1. Key Laboratory of Meteorological Disaster, Ministry of Education / Joint International Research Laboratory of Climate and Environment Change / Collaborative Innovation Center on Forecast and Evaluation of Meteorological Disasters, Nanjing University of Information Science and Technology, Nanjing 210044 China; 2. Chongqing Institute of Meteorological Sciences, Chongqing 401147 China; 3. Key Laboratory for Aerosol-Cloud-Precipitation of China Meteorological Administration, Nanjing University of Information Science and Technology, Nanjing 210044 China; 4.Meteorological Bureau of Xiamen, Xiamen 361012 China)

Abstract: Synoptic systems and microphysical properties associated with a sea fog event are analyzed based on the measurements of visibility, meteorological elements and fog droplet spectrum from a comprehensive field campaign in Xiamen, Fujian province during spring 2013. The influences of meteorological elements on the microstructures of the sea fog are also discussed. The results showed that the wind speed and direction changed suddenly during the intermittent and disperse phases of the sea fog. Liquid water content, number concentration and average diameter varied obviously in the development, mature and disperse phases of the sea fog. The burst re-enforcement of sea fog was accompanied by explosive broadening of fog droplet spectrum; average diameter, number concentration and liquid water content increased sharply; and background meteorological conditions also changed significantly. The microstructures fluctuated intensely due to changes in turbulence, radiation and meteorological conditions at different stages, including nucleation, condensation, coagulation, and evaporation, as well as the discontinuity of spatial distribution of droplets.

Key words: atmospheric physics; sea fog; meteorological elements; microstructure; temporal variation
CLC number: P466 **Document code:** A
doi: 10.16555/j.1006-8775.2017.02.004

1 INTRODUCTION

Sea fog is referred to a condensation phenomenon with visibility less than 1 km in the lower layer over the sea (including the coast and islands). It typically belongs to advective-cooling fog, as a result of synergism of atmospheric radiation, turbulent mixing and advection transmission, which makes relatively warm marine air cool and saturated [1]. Due to high relative humidity, different sizes of droplets interfere with the absorption, reflection and scattering processes of electromagnetic waves in various degrees, which have strong effects on ocean and aerial transportations, industrial and agricultural productions, marine fishing and normal life over the sea or in the coastal areas. Sea fog can also enrich pollutants e and become a hazard to human health.

Fog formation is complex due to many factors, such as atmospheric radiation, particulate matter, the surrounding environment, atmospheric circulation, landscape characteristics, among others[2]. Microphysical properties and visibility are closely related, values of droplet arithmetic mean diameter (D_m), liquid water content (LWC) and number concentration (N) can all directly weaken the effect of visible light [3]. Goodman[4] studied the vertical profiles of microphysical properties of Pacific coastal advection fog, and found that over the peninsula both D_m and LWC of fog droplets (in the 100 m layer above the ground) increased with height during sea fog; the spectrum also appeared to broaden as the sea fog developed toward coastal areas. Hudson [5] investigated the contribution of condensation nuclei to fog microstructures, and found that concentration of fog condensation nuclei and microphysical parameters had certain correlations and that supersaturation could also affect microstructures. Gultepe [6] improved the accuracy of visibility forecasting through applying a new microphysical parameterization for fog visibility in a numerical model.

Zhang[7] found that there were five relatively foggy areas from north to south along the coast of China: waters around Cheng Shantou, Qingdao, the Choushan Archipelago, Leizhou Peninsula and Qiongzhou Strait. Many researchers made observations of sea fogs in

Received 2015-08-15; **Revised** 2017-04-27; **Accepted** 2017-05-15
Foundation item: Natural Science Foundation of China (41675132; 41375138)
Biography: ZHANG Yue, Ph. D., Associate Researcher, primarily undertaking research on marine meteorology.
Corresponding author: FAN Shu-xian, e-mail: shuxianf@nuist.edu.cn

these areas, and had a certain understanding of their climatic characteristics, changes of microphysical properties and droplet distributions. Wang [8] found that sea fog in eastern China usually happens during active warm and moist southerly airflow. Li [9] studied the evolution characteristics of LWC during sea fog, and found that it was not steady or monotonously changing; instead, it had an obvious process of developing-dissipating-redeveloping. Zhou [10] studied the climatic characteristics of spring sea fog over the Yellow Sea. He pointed out that high humidity area was the result of water vapor transport from low latitudes instead of local humidifying.

Xiamen, Fujian province is separated from Taiwan Island and Penghu Archipelago by the Taiwan Strait. It is one of the hubs of comprehensive transportation and an important gateway for foreign trade in China. Sea fogs have strong effects on ocean and aerial transportations and can threaten the safety of travelers. The local economy may suffer heavy losses during a heavy sea fog event. In order to study sea fog evolution and improve sea fog forecast, we chose Dadeng Island as a sea fog field observation site, which is southeast of Xiamen, and carried out a comprehensive meteorological observation of sea fog from March to April in 2013. This article is about the sea fog on 17th April. We analyzed synoptic weather background when the sea fog happened and calculated microphysical properties including N, D_m and LWC. Then, we analyzed the relationships between microstructures and meteorological elements. We also discussed temporal variation characteristics of these microphysical parameters.

2 DATA SOURCES

2.1 *Instrumentation and observation*

The field observation was conducted from 25th March to 25th April 2013 on Dadeng Island (24.33°N, 118.22°E; Fig.1). Instruments were about 1,000 m away from the sea, and at an altitude of 20 m or so.

Figure 1. (a) "A" for Dadeng Island, the observation site; (b): the observation site.

The instruments used in measuring visibility and microphysicsal properties were VPF-30 (Biral, UK) and FM-100 (Droplet Measurement Technologies, USA), respectively. For the meteorological elements (such as temperature, pressure, humidity, wind) on the ground, we used CR3000 open vortex system. The detail refers to Zhang et al.[11].

2.2 *Calculation method*

Methods of calculating microphysical parameters (N, D_m and LWC) are presented in Zhang et al. [11].

Average value (x) and mean squared error $(\sigma(x))$ of microphysical parameters ware calculated using the following formula:

$$x=\sum_1^m \frac{x_i}{m} \quad (1)$$

$$\sigma x=\sum_1^m \frac{(x_i-x)^2}{m} \quad (2)$$

where m is the number of samples, and x is any microphysical parameter under study. Thus, the temporal variation $\delta(x)$ is calculated via the following equation:

$$\delta(x)=\sigma(x)/x$$

3 DESCRIPTION OF FOG PROGRESS

The annual average of fog days was high (40–60 days) during 1971–2010 in Fujian province [12] and this number slowly declined over time due to increase in smog. Sea fogs in Xiamen happen mainly from March to May each year. There were three sea fog events during the observation period, on 15th, 17th and 18th April, respectively.

The lower atmosphere gradually gets warmer in spring. The rising speed of sea surface temperature lags behind that of the surface air temperature; then, the warm air flows over the cold ocean surface and forms an inversion in the lower level. Under such inversion, water vapor from ocean evaporation cannot spread vertically[13]. At 0800 Beijing Time (BT) 17th April, on the 500-hPa height Dadeng Island was in front of a shallow trough, and the temperature trough was behind

the height trough. The front of the trough corresponded to the positive vorticity advection on the ground. Airflow convergence increased in great scope and southwesterly winds brought large amount of water vapor from the sea, promoting the formation and development of sea fog. Visibility (Fig.2a) dropped rapidly from 1313 BT. At 1400 BT, the site was in front of an eastward-moving low-pressure system, and the atmospheric structure was stable. Under the control of the southwesterly airflow, the sea fog formed over the sea surface, moved to Dadeng Island and brought water vapor continuously. The water vapor accumulated in the presence of the associated inversion layer. Heat and moisture exchanged between air and sea violently. Turbulent mixing brought the temperature down in the lower atmosphere. Saturated vapor pressure decreased, and water vapor in the air increased[14].

4 ANALYSIS OF FOG MICROSTRUCTURES

4.1 *Physical cause for each stage*

According to visibility, the sea fog was divided into five stages containing two subprocesses (Fig.2a). Figs.2 and 3 show the changes of meteorological elements and microphysical characteristics during the sea fog. The stages are described as follows:

(1) Stage Ⅰ (preparation of sea fog, from 1313 to 1447 BT 17th April 2013). Visibility reduced quickly from 8.75 km at 1313 BT 17th April. The southwesterly airflow brought a large amount of water vapor. The temperature (T) (Fig.2b) was on the decline and the corresponding saturated vapor pressure decreased, also causing moisture to increase in the atmosphere. As the relative humidity (RH) increased on the ground (Fig. 2b), water vapor condensed on the aerosols and hygroscopic aerosols grew. If the RH is above the critical supersaturation value, the particles will be activated into fog droplets. Wind speed (Fig.2c) continued to fall. Large wind speed would cause strong momentum transportation and turbulence exchange, making the warm upper air mix downward and lower water vapor transfer upward, not favorable for the formation of sea fog [15]. Due to the lack of data before the fog formation, we do not discuss the microphysical characteristics of stage Ⅰ.

(2) Stage Ⅱ (first subprocess of the sea fog, from 1447 to 1731 BT 17th April 2013). Temperature and RH continued to decline and increase, respectively, and wind speed and direction remained, which promoted the development of sea fog. In this stage, the visibility and microphysical parameters were not steady. Microphysical parameters showed quasi-periodic oscillation at a frequency of about 30 minutes, which was determined by dynamic equilibrium of the gravity wave on top of the boundary layer, radiation cooling and turbulent transportation [16]. The temporal variation increased gradually. Drizzles occurred from 1712 BT, raindrops adsorbed fog droplets and aerosols by gravity collision in the process of falling, making N, LWC and D_m decrease sharply and visibility increase.

(3) Stage Ⅲ (the intermittent phase between two subprocesses, from 1731 to 1822 BT 17th April). Visibility improved to more than 1 km. Wind speed kept falling. Turbulent exchange was very weak, to the disadvantage of transport by advection fog. Wind direction changed a little to become the northerly, which meant water in the marine atmospheric boundary provided water vapor for the sea fog rather than local moisture supply. And the atmospheric circulation created a favorable condition for advection transport of warm and moist air [10]. Temperature stopped falling, but

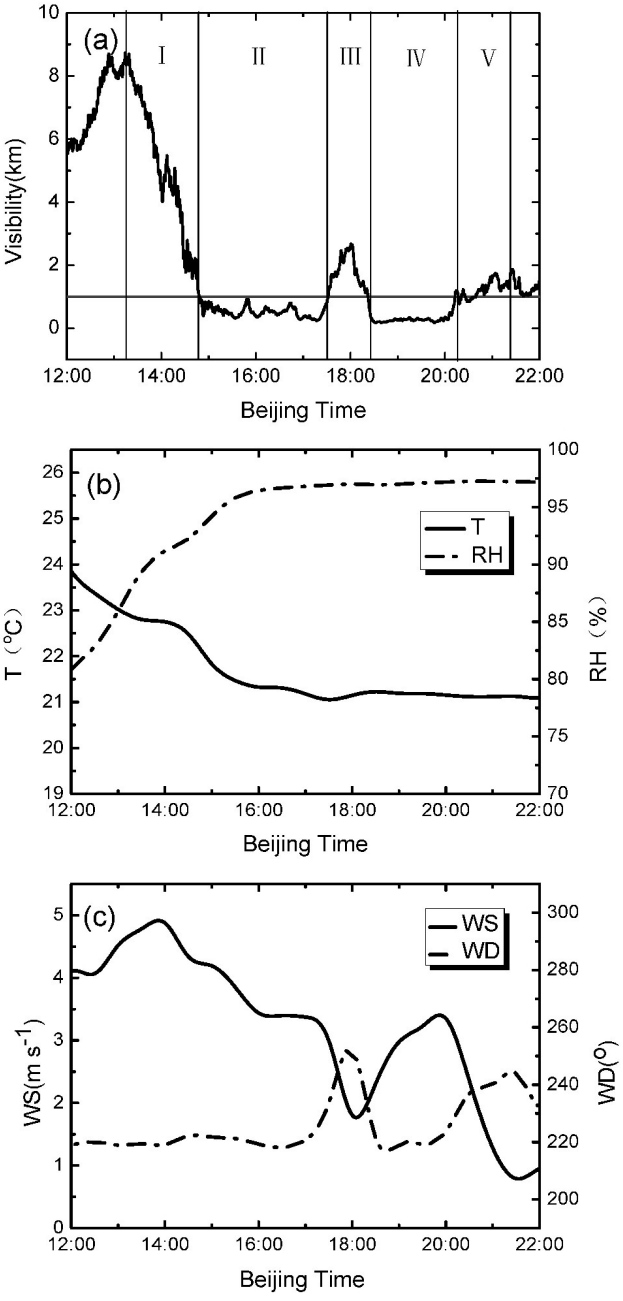

Figure 2. Temporal evolutions of (a) visibility; (b) temperature (T) and humidity (RH); and (c) wind speed (WS) and wind direction (WD).

maintained steady due to the increase of downward longwave radiation with the appearance of the sea fog and latent heat release by water-vapor condensation [17]. N, LWC and D_m remained at low values. So, visibility sharply recovered and reached its maximum around 1800 BT when the wind returned to the easterly accompanied with gradually increasing wind speed. Drizzle stopped. So, in the later part of the intermittent stage, microphysical parameters began to increase and visibility dropped quickly.

(4) Stage **IV** (second subprocess, from 1822 to 2011 BT 17th April). The second dense fog appeared; N, LWC and D_m grew explosively. This process will be described in detail in the following pages. Same as the first subprocess, microphysical parameters showed quasi-periodic oscillations. Explosive growth of the sea fog demonstrated that both nucleation and coagulation were important. Afterwards, LWC and D_m declined somewhat and fluctuated smoothly after 1900 BT. The sea fog developed rapidly, visibility maintained at a lower level.

(5) Stage **V** (disperse phase, from 2011 to 2125 BT 17th April). The sea fog began to dissipate, and the wind started to decline. The airflow turned to the northerly. Visibility showed ups and downs during the dissipation process. LWC, N and D_m fell to their equilibrium values. The sea fog process was over at 2125 BT.

In general, the microphysical parameters changed sharply during the fog event, even fluctuated during the same stage. It shows that microphysical structures of sea fog were inhomogeneous in space and time. Time variation of visibility was opposite to those of N, LWC and D_m. The temporal variation of N was most energetic. The temporal variations of LWC and N were basically the same. It shows that droplet number concentration led to the change of LWC during the sea fog. In the stages of formation, intermission and disperse, N, LWC and D_m were usually small and fluctuated slightly. Stability of the wind was very important for the formation of sea fog and maintenance[18]. During the two subprocesses, the range of D_m was 5 –12 μm, which means coagulation played an important role.

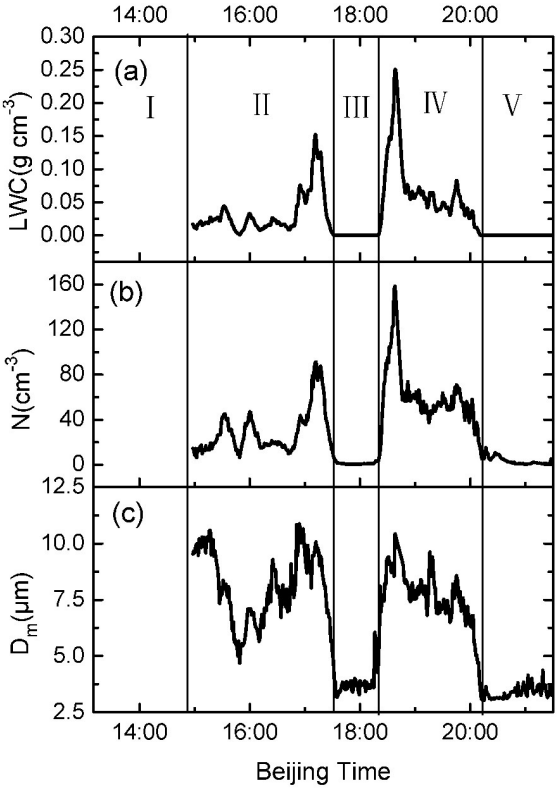

Figure 3. Temporal variations of (a) LWC, (b) N and (c) D_m.

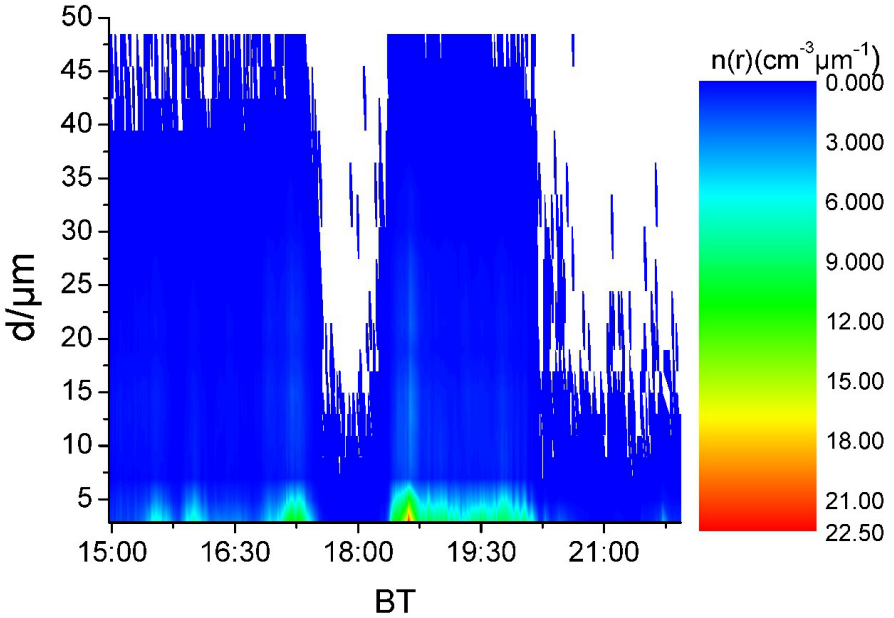

Figure 4. Temporal evolution of spectra.

4.2 *The burst broadening of droplet spectra*

From Fig.4, the droplet spectra explosively broadened around 1820 BT. The droplet number density increased rapidly and subsequently droplet spectra appeared broadening significantly. Droplets coagulation consumed small droplets; however, small droplet number density increased, as in the observations of Liu [19] and Niu [20]. Adequate water vapor and condensation nuclei led to strong nucleation and condensation, which produced sufficient new droplets to make up for the loss by coagulation[20]. From the microphysical characteristics shown in Fig.3, D_m changed first. N and LWC grew rapidly with the dramatic increase in D_m. Visibility dropped sharply. LWC, N and D_m reached their peaks almost at the same time around 1835 BT.

Table 1 shows the changes of microphysical parameters and meteorological elements before and after the explosive increase of fog. Through nearly 30 minutes of explosive development, visibility suddenly changed from 2.63 km to 200 m, N and LWC increased by two orders of magnitude, D_m increased twice, and spectral width expanded from 15 to 50 μm. In terms of macroscopic meteorological elements, the wind direction varied from the relatively dry continental air mass to marine wind with sufficient water vapor. The wind speed increased twice. A steady stream of water vapor was brought to the island and turbulent mixing enhanced; meanwhile, longwave radiation strengthened after sunset, and the nucleation and condensation of droplets enhanced with coagulation. Droplet spectra broadened explosively[21].

Table 1. Changes of microphysical parameters, visibility, WD, WS, and T before and after the bursting broadening.

Burst time	N(cm^{-3})	LWC(g m^{-3})	D_m(μm)	Dmax(μm)	Visibility(km)	WD(°)	WS(ms^{-1})	T(℃)
Start 18:00	0.58	0.001	3.90	14.97	2.63	250	1.6	21.15
End 18:35	121.79	0.178	9.12	48.48	0.2	220	3.2	21.25

5 ANALYSIS OF TEMPORAL VARIATION CHARACTERISTICS OF FOG MICROSTRUCTURES

5.1 *Temporal variations of meteorological fields and microphysical characteristics*

We noticed that the temporal and spatial distribution was very uneven throughout the whole evolution of the sea fog. Visually observed fog changed frequently, being heavy or light alternatively. From the calculation results, we can see changes of N, D_m and LWC varied at different stages by as much as 1 –2 orders of magnitude. The fluctuations of fog microstructures would significantly affect the growth of droplets. Temporal variations of meteorological fields including that of microphysical characteristics themselves needed to be considered. We can understand the actual situation of fog microstructures more comprehensively and the fog development better by studying their statistical characteristics[22].

Figures 5 and 6 describe the temporal variations of meteorological parameters and microphysical parameters averaged during each minute, respectively. LWC and N were almost zero in the stages of intermittency and disperse, so no future discussion is needed. Due to the relationship between D_m and N, we also do not need to discuss the temporal variation of D_m, once we know that of N.

Temperature can affect the formation of new particles and the growth of particles, and supersaturation is the prerequisite of aerosol activation. Therefore, the variations of temperature and supersaturation must influence the temporal variations of D_m, LWC and N[23]. Wind direction is important for the external source of water vapor, and the change of wind speed determines the conveying and mixing of water vapor and droplet evaporation. As a result, both wind speed and direction can affect temporal variations of the microstructures. Fig.5 shows that the temporal variation of vertical wind velocity was much larger than that of horizontal wind

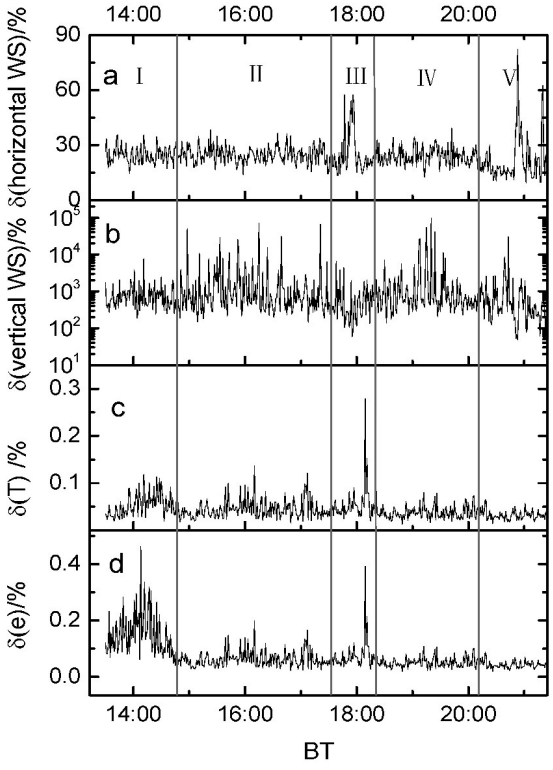

Figure 5. Temporal evolutions showing the fluctuations of (a) horizontal wind, (b) vertical wind speed, (c) *T*, and (d) water vapor pressure (e).

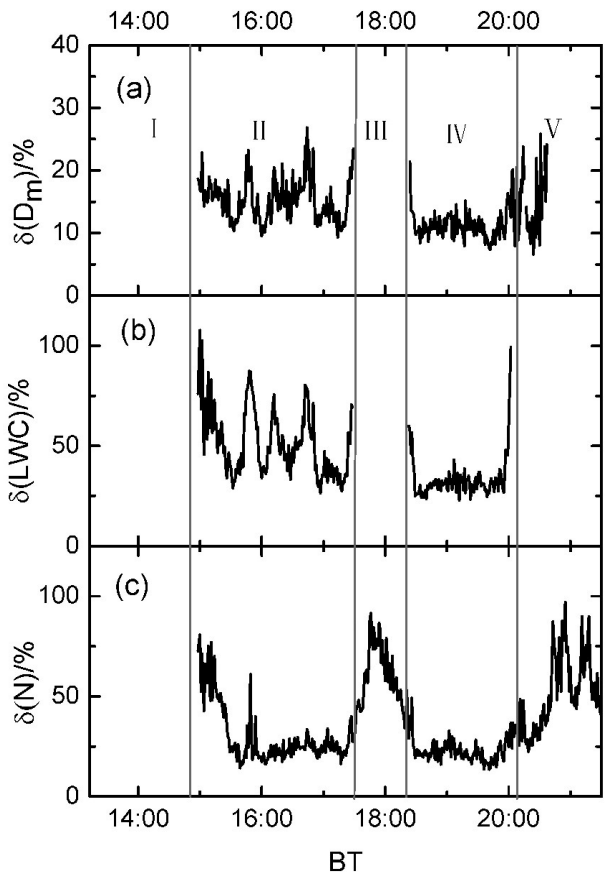

Figure 6. Temporal evolutions of (a) D_m, (b) LWC and (c) N.

speed. Temporal variation magnitudes of temperature and vapor pressure were small. Nevertheless, in the development period of the first subprocess, turbulence was enhanced during the variations of temperature and vapor pressure. This is because fog droplets released latent heat when they condensed and grew. In the intermittent stage, there were bursts of temporal variations of horizontal wind speed, temperature and vapor pressure. Explosive temporal variation was only found in horizontal wind speed in the disperse phase.

Environmental conditions in sea fog, such as flow field and temperature, were nonhomogeneous. Condensation growth with fluctuations could produce different sizes of fog droplets. Temporal variations of LWC, turbulent acceleration and updraft led to different condensation growth in the fog area. Moreover, random distribution of fog droplets caused discontinuous coagulation. D_m fluctuated with size spectrum, making LWC go up and down[22].

From Fig.6, in every minute, all microphysical parameters fluctuated to different extents. Temporal variation of LWC was the largest, between 40% and 110% per minute. Temporal variation of N took the second place, between 30% and 100% per minute. Temporal variation of D_m was the least, between 5% and 25% per minute. LWC in sea fog depended on droplet number concentration and diameters of big fog droplets. Overall, temporal variation in stage **IV** was less than that in stage **II**. Stage **II** was mainly the development phase of the first subprocess, and stage **IV** was mainly the mature phase of the second subprocess; so, the fog layer was relatively more stable during its mature phase.

Temporal variation curve of LWC was similar to that of D_m, which shows that the temporal variation of LWC was mainly controlled by that of D_m. The temporal variation of N was small during the first and second subprocesses. Steady southwesterly wind brought sufficient water vapor to contribute to the activation and condensation of droplets, combined with gravity settling of big fog drops with continuous nucleation, condensation and coagulation of small fog droplets, accounting for the smooth temporal variation. In the intermittent and disperse phases, temporal variation was more apparent, while wind speed and direction changed suddenly, especially when drizzles occurred in stage **III**; this brought about random changes in visibility and microphysical characteristics. It shows that macro meteorological elements had strong influences on the changes of microstructures of sea fog [23]. Relationships between temporal variation of microphysical parameters and microphysical parameters themselves were not apparent. Sometimes, microphysical parameters increased sharply over time, but the temporal variations were not obvious. Microphysical parameters of Dadeng Island's sea fog were not only related to the uniform fog layer structure itself but also to the effects of environment factors. There are hills and buildings of various heights in Dadeng Island. Sea fog moved with the air flow from the sea surface, whose underlying surface was relatively uniform, to uneven land surface, associated with irregular climbing and circumferential motions; all these made microstructures inhomogeneous and oscillating in time [24]. The observational data was collected at the bottom of the inhomogeneous fog. Characteristics of turbulent statistics differed at different heights. So, temporal variations at the middle and upper levels differed from those at the bottom.

5.2 *Relationship between average wind speed and temporal variations of microphysical characteristics*

During the sea fog, temporal variations of LWC, N and D_m were not the same in any given minute, neither were the changes of their one-minute averages over time (Fig.7a, b, c). D_m, and its temporal variation (Fig.7a) were not correlated; temporal variations of LWC and N were large but their one-minute average values were small, which shows that temporal variations of LWC and N had certain negative correlations with their one-minute averages. The relationship was opposite to the observational results by Xu[25] in Hengshan, in which the temporal vatiations of microparameters and their averages had certain positive correlation. Because of the every-improving instruments, every set of observations taken in Hengshan was separated from the next set by a

few hours. During each time interval (gap), the fog had different degree of development, evolutions of the microphysical structures could not be completely recorded. Moreover, the temporal variation of air in the instrumental air-intake tunnel caused ups and downs of captured cloud droplets and airflow rate, causing large errors in the data. The sampling frequency of a fog particle spectrometer was set to 1 Hz in Dadeng Island. The temporal variation intensities of microphysical parameters and their one-minute averages were calculated. Determination of particle diameter size by measuring the scattering light intensity of droplets was based on the Mie scattering theory, and particle diameter sizes were grouped into different ranges, making data more complete and accurate. From Fig.7b, the LWC of droplets fluctuated strongly while its values

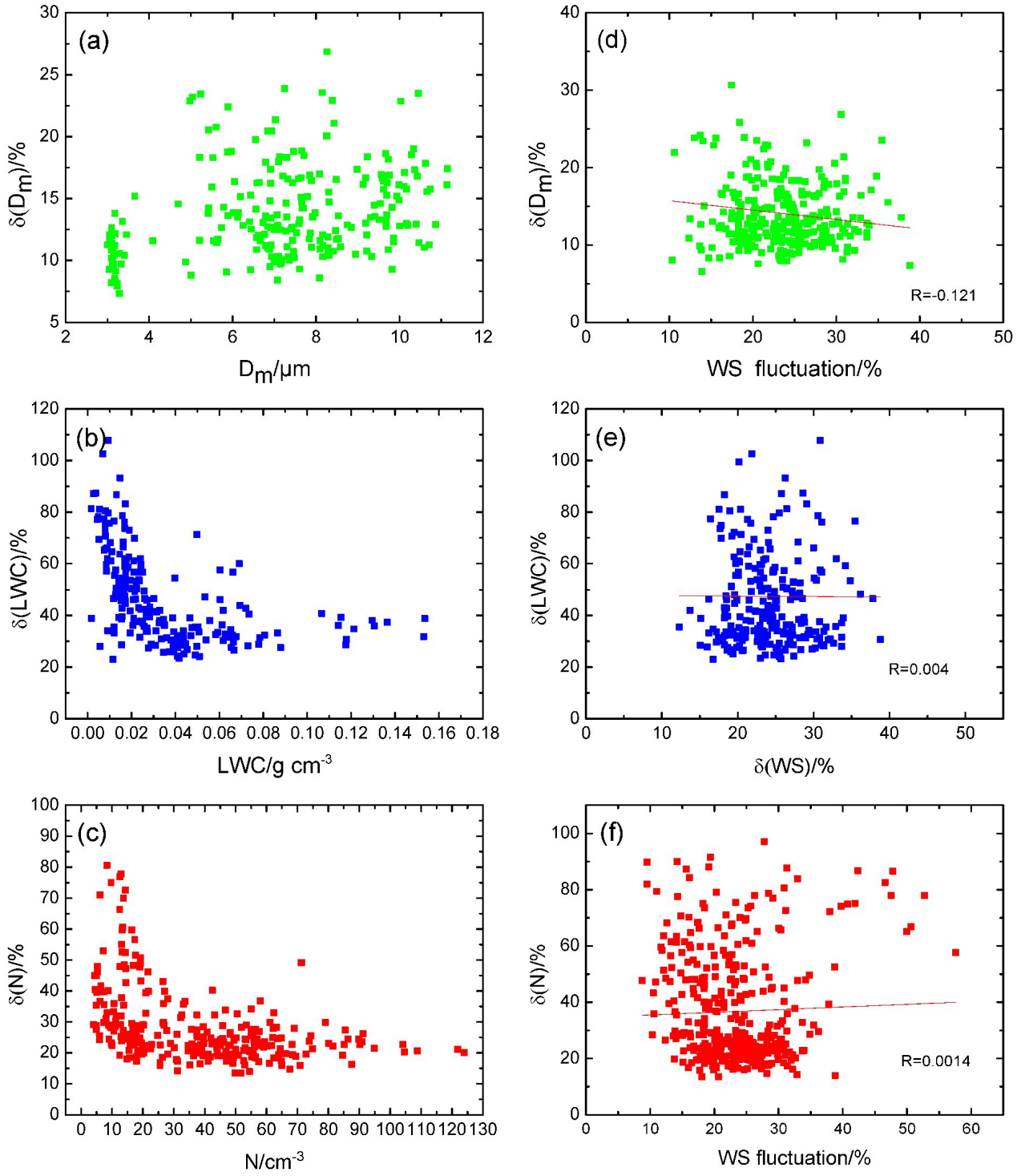

Figure 7. Relationships between (a) temporal variation of D_m and its one-minute average, (b) temporal variation of LWC and its one-minute average, (c) temporal variation of N and its one-minute average, (c) temporal variation of D_m and temporal variation of WS, (d) temporal variation of LWC and temporal variation of WS, and (e) temporal variation of N and temporal variation of WS.

were small. Fig.7c shows that the N of droplets also had this feature. Besides, small temporal variations of LWC and N corresponded to the mature phase of sea fog, although temporal variations of LWC, N and D_m did not show close relationships with temporal variation of wind speed (Fig.7d, e, f). When the wind speed changed, N changed violently, and the development of the fog also changed. So, we cannot simply use inverse correlations to describe relationships between temporal variation intensities of LWC and N and their one-minute averages. They had no relationships. Temporal variation intensities of microphysical parameters are mainly associated with the development of the sea fog. The sea fog was advection fog and relied on the movement of air. The change of wind direction and discontinuous air transportation made the sea fog change violently. The macroscopic and microscopic physical processes were closely linked, and influenced each other during sea fog; so, it is necessary to consider the combination of macroscopic and microscopic physical processes when studying the changes in microphysical structures and their fluctuations.

5.3 *Temporal variations of concentration of different size droplets*

Movements of fog droplets due to the airflow were affected by their diameters, which was caused by inertia. Hence, when we analyze temporal variations of different size droplet concentration, we divide the diameters into the following ranges according to the sizes of the diameters (there were extreme values around 10 μm and 20 μm) combined with the range of the instrument: 2 μm < D < 10 μm, 10 μm < D < 20 μm, and 20 μm < D < 50 μm. On the basis of the three ranges, we calculated their concentration (temporal) variations separately. Fig.8 shows the temporal variation intensity of number concentration averaged over each minute. The concentration of fog droplets bigger than 10 μm was almost zero in the intermittent and disperse stages; so, we do not discuss them here.

Figure 8 shows that the concentration variation of large droplets (20 μm < D < 50 μm) was the largest and that the concentration variation of small droplets (D < 10 μm) was the smallest, which means the nucleation process was active in each stage. Bigger droplets had stronger gravity settling, while smaller drops condensed and coagulated randomly. As a result, the larger the diameter, the more violent the temporal variation. Concentration variation of D < 10 μm was similar to that of the total number in Fig. 8c, showing that small droplets made the most contribution to the sea fog. In stages **II** and **IV**, the concentration variation of droplets D < 10 μm was steady, showing that the growth rate of small droplet activation was weak during the development of sea fog. In the intermittent and disperse stages, small droplets fluctuated more intensely, meaning that activation growth of small droplets was effected by environmental meteorological elements such as wind. The concentration variation of larger droplets

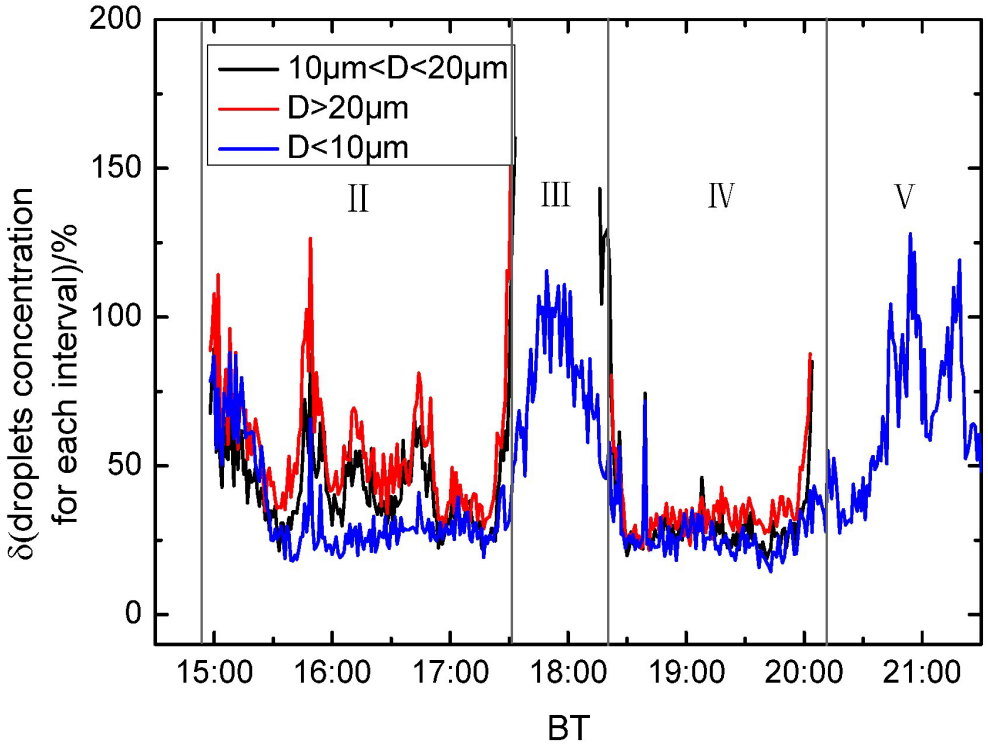

Figure 8. Temporal evolution showing the temporal variation of droplet number concentration for each range (blue: 2 μm < D < 10 μ m, black: 10 μm < D < 20 μm, and red: 20 μm < D < 50 μm).

(10 μm < D < 20 μm) and largest droplets (20 μm < D < 50 μm) oscillated in stage Ⅱ, but relatively steady in stage Ⅳ. Fog structure in stage Ⅳ was more mature and stable than that in stage Ⅱ, showing that the number concentration variation of D > 10 μm was closely related with the development degree of sea fog. Changes of temporal variation intensity of droplet number concentration show that nucleation, condensation, coagulation, and evaporation in sea fog made fog droplet concentration change all the time[26].

5.4 *Analysis of temporal variation characteristics of droplet spectra*

Figure 9 shows the distribution curve of droplet spectra in each stage and describes the trends of droplet spectral width and number concentration. Number density distribution fluctuated over time. Number density of each stage decreased on the whole. Decreasing speed gradually slowed down with the increasing of the droplet diameter. Spectrum was wide in each stage. Spectral curves of stages Ⅱ and Ⅳ were obviously higher than those of stages Ⅲ and Ⅴ. Compared to the development and mature phases of the first subprocess (Ⅱ), wind direction changed and wind speed decreased in the intermittent phase (stage Ⅲ), and the droplet spectral curve fell significantly. The number densities of different size droplets were significantly lower than those in stage Ⅱ. Due to the drizzles, raindrops absorbed aerosols in the process of falling. But, the spectral width did not narrow in stage Ⅲ. Moreover, the number concentration of large droplets fluctuated because of continuous coagulation. In the second subprocess (stage Ⅳ), the wind direction and speed changed again, and visibility reduced to less than 1 km. Compared to stage Ⅱ, the spectral distribution was similar and the spectral curve was slightly higher, which means the nucleation and growth processes in the second subprocess were more intense than those in the first subprocess, causing visibility to be lower generally in the second subprocess. During the disperse phase (stage Ⅴ), there was still a sudden change of wind direction and wind speed, the spectral curve significantly decreased. Compared to the intermittent phase, the curve lifted where the diameter is less than 6 μm while the curve dropped rapidly where the diameter is larger than 6 μm. Spectral width narrowed accordingly, which shows that drizzles had big effects on the small droplets in the intermittent phase. The lack of water source in stage Ⅴ, besides gravity settling of large droplets and evaporation process, reinforced, owing to weakened wind speed, which led to the disappearance of sea fog. The physical processes in the sea fog made droplet spectra vary, depending on the dynamic and thermal environments of occurrence and maintenance of sea fog. Droplet spectra can also well reflect the physical process in sea fog[27].

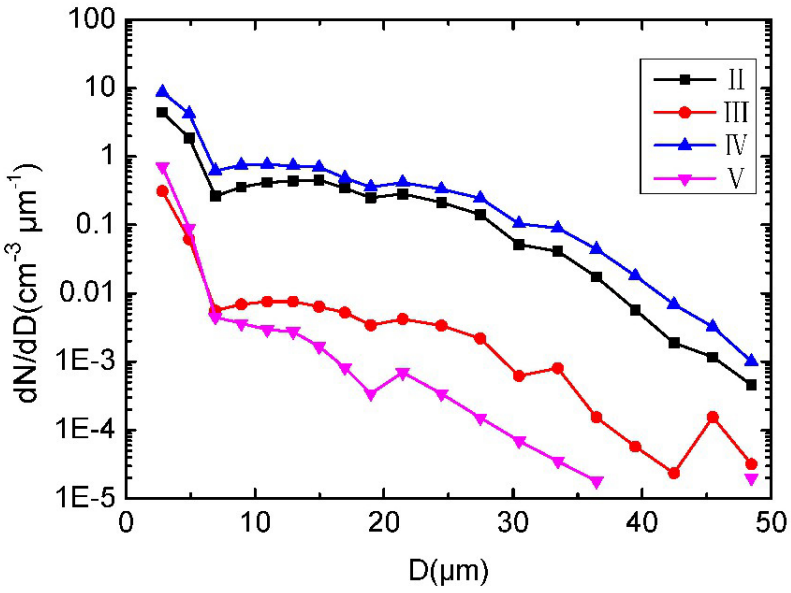

Figure 9. Drop-size distributions at various stages of the sea fog.

6 RESULTS

Based on the data of visibility, conventional meteorological elements and droplet spectra during a sea fog on 17th April 2013 in Xiamen, Fujian province, we analyzed weather systems, weather conditions and temporal variation characteristics of the microstructures.

(1) The sea fog happened in front of an eastward moving low pressure on the ground. The wind was mostly weak and from southwest in the process of the sea fog, and brought a steady stream of water vapor. High altitude was affected by a shallow trough.

(2) In different stages, microphysical characteristics had obvious differences. Even in the same stage, microphysical parameters fluctuated and showed quasi-periodic oscillations. Wind speed and direction changed suddenly in the intermittent phase and disperse phase.

(3) In the process of explosive increase of sea fog, the droplet spectra widened explosively. From the physical structures, average diameter took the lead to grow, with number density and LWC increasing suddenly. At the same time, macro meteorological conditions (wind direction, wind speed) also changed.

(4) Due to differences in turbulence, radiation and meteorological conditions, plus the discontinuous distribution of droplets, nucleation, condensation, coagulation, and evaporation, the ups and downs of microstructures changed substantially. The temporal variation intensities of microphysical parameters had little to do with their one-minute average values or the wind speed temporal variation, but were associated with the development process of the sea fog.

(5) Number concentration variation of the small droplets was similar to that of the total number concentration. Randomicity of gravity settling, condensation and coagulation of larger droplets increased their temporal variations.

(6) Droplet distribution curve showed the trend of rising and falling along with the development of the sea fog, as well as with the change of the spectral width.

REFERENCES:

[1] WANG Bin-hua. Sea Fog [M]. Beijing: Ocean Press, 1983: 180-254 (in Chinese).

[2] GULTEPE I, TARDIF R, MICHAELIDES S, et al. Fog Research: A review of past achievements and future perspectives [J]. Pure Appl Geophys, 2007, 164 (6): 1121-1159.

[3] ELDRIDGE R G. The relationship between visibility and liquid water content in fog [J]. J Atmos Sci, 1971, 28(7): 1183-1186.

[4] GOODMAN J. The microstructure of California Coastal fog and stratus [J]. Appl Meteorol, 1977, 16 (10): 1056-1067.

[5] HUDSON J G. Relationship between fog condensation nuclei and fog microstructure [J]. Atmos Sci, 1980, 37(8): 1854-1867.

[6] GULTEPE I, MILBRANDT J. Microphysical observations and mesoscale model simulation of a warm fog case during FRAM project [J]. Pure Appl Geophys, 2007, 164 (6): 1161-1178.

[7] ZHANG Su-ping, BAO Xian-wen. Sea fog research in China in the last ten years [J]. J Ocean Univ China, 2008, 38(3): 359-366 (in Chinese).

[8] WANG Ya-nan, LI Yong-ping. Analysis of characteristics of sea fog of the Yellow Sea and East China Sea under the influence of cold air [J]. J Trop Meteorol, 2009, 25 (2): 216-221 (in Chinese).

[9] LI Xiao-na, HUANG Ji'an, SHEN Shuang-he, et al. Evolution characteristics of liquid water content in a high pressure sea fog [J]. J Trop Meteorol, 2010, 26(1): 79-85 (in Chinese).

[10] ZHOU Fa, WANG Xin, BAO Xian-wen. Climate characteristics of sea fog formation of Yellow Sea in spring [J]. Acta Oceanol Sinica, 2004, 26 (3): 28-37 (in Chinese).

[11] ZHANG Shu-ting, NIU Sheng-jie, ZHAO Li-juan. The microphysical structure of fog droplets in a sea fog event in the South China Sea [J]. Chin J Atmos Sci, 2013, 37 (3): 2012-2024 (in Chinese).

[12] SU Yu, MA Zhen-feng, NIU Tao, et al. Climate change characteristics of fog days and haze days in China in recent 40 years [J]. Clim Environ Res, 2013, 18 (3): 397-406 (in Chinese).

[13] HU Rui-jin, DONG Ke-hui, ZHOU Fa, et al. Numerical experiments of advection, turbulence and radiation effects in the progress of sea fog formation [J]. Adv Marine Sci, 2006, 24(2): 282-292 (in Chinese).

[14] HU Zhao-xia, LEI Heng-chi, DONG Jian-xi, et al. Analysis of characteristics and numerical simulation in a sub-regional warm fog [J]. Clim Environ Res, 2011, 16 (1): 71-84 (in Chinese).

[15] YUE Yan-yu, NIU Sheng-jie, ZHAO Li-juan, et al. Study on the synoptic system and macro-micro characteristics of sea fog along the Zhanjiang coastal area [J]. Chin J Atmos Sci, 2013, 37(3): 609-622 (in Chinese).

[16] SHEN Chen, HUANG Jian, LIU Shou-dong. Quasi-periodic oscillation characteristics of sea fog [J]. J Trop Meteorol, 2010, 26(1): 71-78 (in Chinese).

[17] HE Hui, GUO Xue-liang, LIU Jian-zhong, et al. Observation on the boundary structure characteristics and mechanism of formation-elimination and numerical simulation in a sea fog event in Beijing [J]. Chin J Atmos Sci, 2009, 33(6): 1174-1186 (in Chinese).

[18] HUANG Bin, MAO Dong-yan, KANG Zhi-ming, et al. Analysis of climate characteristics and cause of formation of sea fog in the Yellow Sea [J]. J Trop Meteorol, 2011, 27(6): 920-929 (in Chinese).

[19] LIU Lin-wei, NIU Sheng-jie, LIU Duan-yang, et al. Evolution characteristics and explosive enhance research during winter fog events in Nanjing [J]. J Atmos Sci, 2012, 35(1): 103-112 (in Chinese).

[20] NIU Sheng-jie, LU Chun-song, LIU Yan-gang, et al. Analysis of the microphysical Structure of heavy fog using a droplet spectrometer: A case study [J]. Adv Atmos Sci, 2010, 27(6): 1259-1275.

[21] LIU Duan-yang, YANG Jun, NIU Sheng-jie. On the evolution and structure of a radiation fog event in Nanjing [J]. Adv Atmos Sci, 2011, 28(1): 223-237.

[22] GU Zhen-chao. Basis of cloud-fog-precipitation physics [M]. Beijing: Science Press, 1980: 36-58 (in Chinese).

[23] LIU Peng-fei, ZHAO Chun-sheng, GOBELl T, et al. Hygroscopic properties of aerosol particles at high relative humidity and their diurnal variations in the North China Plain [J]. Atmos Chem Phys, 2011, 11 (1): 3479-3494.

[24] TANG Hao-hua, FAN Shao-jia, WU Dui, et al. Microphysical characteristics and evolution progress of a dense fog in Nanling Mountain [J]. J Sun Yat-sen Univ (Nat Sci Edit), 2002, 41(4): 92-96 (in Chinese).

[25] XU Huan-bin. Preliminary observation of microstructure of cloud-fog in Heng Mountain[J]. Acta Meteorol Sinica,

1964, 34(4): 539-547 (in Chinese).
[26] HUANG Hui-jun, HUANG Jian, LIU Chun-xia, et al. Microphysical characteristics of sea fog in Maoming region [J]. Acta Oceanol Sinica, 2009, 31 (2): 17-24 (in Chinese).
[27] QU Feng-qiu, LIU Shou-dong, YI Yan-ming, et al. Analysis of a fog event in South China [J]. J Trop Meteorol, 2008, 24(5): 490-496 (in Chinese).

Citation: ZHANG Yue, FAN Shu-xian, ZHANG Shu-ting et al. Microstructures and temporal variation characteristics during a sea fog event along the west coast of the Taiwan Strait [J]. J Trop Meteorol, 2017, 23(2): 155-165.